# Recent advances in three-dimensional large-scale electromagnetic modeling and inversion

Michael S. Zhdanov[1,2], Masashi Endo[1], Leif H. Cox[1], and Martin Čuma[1,2]
[1]TechnoImaging, Salt Lake City UT
[2] Consortium for Electromagnetic Modeling and Inversion, University of Utah, Salt Lake City UT

## SUMMARY

This paper reviews recent advances in 3D EM modelling and inversion, based on integral equation (IE) method. While the basic theory of the IE method has long been established, advances in algorithms, software engineering, and computing resources have significantly expanded the IE method's capabilities and applications. We demonstrate in this paper how the IE method can simulate the same model complexity as finite-difference (FD) or finite-element (FE) methods, while providing efficient inversion algorithms. We present the case studies for the inversion of the marine and airborne EM data for very large-scale 3D earth models.

**Keywords**: 3D, electromagnetic, modeling, inversion, integral equations, large-scale.

## INTRODUCTION

For nearly forty years, the integral equation (IE) method has been a powerful method for 3D EM modeling and inversion. The principles of IE method were formulated practically simultaneously in the papers by Raiche (1974), Weidelt (1975), and Hohmann (1975). Over the last thirty years, generations of EM modellers have contributed to the development of the IE method (e.g., Wannamaker, 1991; Dmitriev and Nesmeyanova, 1992; Xiong, 1992; Xiong and Tripp, 1994; Singer and Fainberg, 1995; Avdeev et al., 1997, 2002; Hursán and Zhdanov, 2002; Zhdanov et al., 2006).

The main advantage of the IE method when compared to the various finite-difference (FD), or finite-element (FE) methods is the fast and accurate simulation of EM data for models of compact 3D targets embedded in layered backgrounds. Traditional implementations of the IE method result in small but full linear systems that can be solved using direct methods. However, the governing equations of the IE method can also be considered as convolutions of the Green's tensors and scattered currents, meaning the linear system can be decomposed to Toeplitz or block-Toeplitz structures. For iterative solvers, this means 2D FFT convolutions can be used for fast matrix-vector multiplications, resulting in a significant decrease in runtimes compared conventional implementations of iterative solvers (Hursán and Zhdanov, 2002). Further, the multiple-domain IE (Endo et al., 2009) enables this method to be applied to the computation for models with the same complexity as FD or FE methods. Finally, implementation of the moving sensitivity domain makes practical the inversion of extremely large scale land, marine, and airborne EM surveys (Cox and Zhdanov, 2007; Cox et al., 2010; Zhdanov et al., 2011a, 2011b, 2011c, 2012).

## INTEGRAL EQUATION MODELING

It is well known that we can derive a vector Fredholm integral equation of the second kind for the scattered electric fields for the model domain D:

$$\mathbf{E}^s(\mathbf{r}') = \int_V \widehat{\mathbf{G}}_E(\mathbf{r}',\mathbf{r})\, \Delta\sigma(\mathbf{r})[\mathbf{E}^b(\mathbf{r}) + \mathbf{E}^s(\mathbf{r})]dv, \qquad (1)$$

where $\widehat{\mathbf{G}}_E(\mathbf{r}',\mathbf{r})$ is the body-to-body electric Green's tensor for the background conductivity model. Anisotropic conductivity is easily introduced via the background conductivity model, $\sigma_b(z)$, and subsequent background electric field and Green's tensor evaluations. The volume integration is only evaluated over those cells in the model where the conductivity differs from the background conductivity. The advantage of the IE method over the various FD, FV, or FE methods is that the entire 3D earth model need not be discretized with an appropriate choice of boundary conditions so as to emulate an unbound 3D earth model. Rather, an appropriate background conductivity model is chosen, and only the volume of interest is discretized, with all boundary conditions perfectly matched. This means that we can simultaneously solve equation (1) for $N_D$ multiple domains:

$$\mathbf{E}^s(\mathbf{r}') = \sum_{i=1}^{N_D} \int_V \widehat{\mathbf{G}}_E(\mathbf{r}',\mathbf{r})\, \Delta\sigma(\mathbf{r})[\mathbf{E}^b(\mathbf{r}) + \mathbf{E}^s(\mathbf{r})]dv, \quad (2)$$

where all of the domains are fully coupled. Each domain may be of different dimensions and/or discretization. For example, in marine EM applications, we may finely discretize one domain for the bathymetry, have another coarsely discretized for regional (background) sedimentary structures, and finely discretize a third domain incorporating the reservoir formations of interest. This is the basis of the multi-domain (Endo et al., 2009) and inhomogeneous background conductivity (Zhdanov et al., 2006) algorithms for the IE method. Using the method of moments, equation (2) can be reduced to the linear system:

$$(\mathbf{I} - \mathbf{\Gamma} \cdot \Delta\boldsymbol{\sigma})\mathbf{E}^s = \mathbf{\Gamma} \cdot \Delta\boldsymbol{\sigma} \cdot \mathbf{E}^b, \quad (3)$$

where $\mathbf{E}^s$ is the vector of the scattered electric fields, $\mathbf{I}$ is the identity matrix, $\mathbf{\Gamma}$ is the matrix of volume-integrated body-to-body electric Green's tensors for the background conductivity model, and $\Delta\boldsymbol{\sigma}$ is a diagonal matrix of anomalous conductivities. Equation (2) requires the total electric field in each cell, and this is computed as the sum of the background and anomalous electric fields. For high conductivity contrasts, this can propagate numerical errors due to the finite precision of adding numbers of similar amplitude but opposite sign. By adding the background electric fields to both sides of equation (3) and after some algebra, we can instead obtain the linear system:

$$(\mathbf{I} - \mathbf{\Gamma} \cdot \Delta\boldsymbol{\sigma})\mathbf{E} = \mathbf{E}^b, \quad (4)$$

which directly solves for the total electric field, $\mathbf{E}$, instead of the scattered electric field, $\mathbf{E}^s$, while retaining the distributed source in terms of the background electric fields, $\mathbf{E}^b$. This is a unique property of IE methods and their hybrids. That said, equation (4) requires the solution of a large, dense, and ill-conditioned matrix system. Following Hursán and Zhdanov (2002), we pre-condition equation (4) with contraction operators to improve the conditioning of the matrix system. We can then write equation (4) in the form:

$$\hat{\mathbf{L}}\mathbf{E} = \mathbf{e}, \quad (5)$$

where $\mathbf{E}$ and $\mathbf{e}$ are the vectors of preconditioned total and background electric fields, respectively. As shown by Hursán and Zhdanov (2002), if the anomalous domains are discretized into an $N_x \times N_y$ horizontally homogeneous array of cells, the scattering matrix has a block Toeplitz structure. Specifically, this means the number of unique Green's tensor kernels (which comprise $\mathbf{\Gamma}$) is $N_x \times N_y$ times smaller than the number of elements in $\mathbf{\Gamma}$. This provides for the economic storage of $\mathbf{\Gamma}$, and avoids historic memory limitations associated with storing the full (and redundant) $\mathbf{\Gamma}$. Further, we can recognize that equation 2 represents a convolution of the Green's tensors with the scattered current. Thus, equation (5) can be represented as a series of discrete 2D convolutions followed by summation over the vertical discretization. In scalar notation, we can write this as:

$$e_{\alpha i} = \sum_{\beta=x,y,z} \sum_{n=1}^{N_z} \left(\ell_{\alpha i \beta n} * E_{\beta n}\right) \quad (6)$$

where $\ell_{\alpha i \beta n}$ is an array storing all different nonzero scalar components of $\hat{\mathbf{L}}$, $\alpha$ and $\beta$ are the indices of the corresponding scalar components of $\mathbf{E}$, $i$ and $n$ are the indices of the source and receiver positions along the vertical axis in the expression for the Green's tensor, and the asterisk ($*$) denotes a discrete 2D convolution in the horizontal plane. We can then apply the discrete convolution theorem:

$$\ell_{\alpha i \beta n} * E_{\beta n} = FFT^{-1}\left[FFT(\ell_{\alpha i \beta n}) \cdot FFT(E_{\beta n})\right]. \quad (7)$$

The advantage of equation (7) is that we replace the direct matrix multiplication with fast Fourier transforms (FFT), reducing the operation complexity from $O(N^2)$ to $O(N\log N)$, where $N = N_x \times N_y$. This is very advantageous for iterative solvers. In particular, we use the complex generalized minimum residual method (CGMRES) method as a solver for linear system (6), because this method has been proven convergence (Zhdanov, 2002).

Equation (7) can be parallelized over three levels. The first is over frequency, and the second is over the sources. These two are easy to implement, as they are simply distributions over different sets of processor units (PUs). The third level is over the model domain. However, parallel computing libraries, generally, are not optimized for solving equation (7), as the parallel FFT is one of the most difficult operations on shared memory parallel architectures. To overcome this, we use a 1D block cyclic distribution which has good memory access in the serial order in each PU. Note that the performance depends on the costs of the FFT and of the interprocessor communications. This balance can be changed by optimizing the code and hardware, and the size of the modeling grid.

Relative to modeling, inversion subroutines consume considerably less time and resources. Yet, for optimization, inversion subroutines are also parallelized over the $z$ discretization. The domain $z$ layers are distributed to the processors in sequential order, each PU having the number of $z$ layers equal to the total number of $z$ layers in the inversion domain ($N_z$). All inversion data structures that span the model domains (e.g., model weights, conductivities, Frechet derivatives, etc) are distributed in this manner. Each PU holds in its memory and evaluates only the $z$ layer assigned to it. As there is minimal inter-cell dependence on the evaluation of the model domain data, the inversion subroutines use only a limited amount of communication to evaluate the minimization step length.

## CASE STUDIES

IE methods have been applied to all EM modeling and inversion problems, including airborne EM (Cox et al., 2010), marine EM (e.g., Zhdanov et al., 2011a, 2011b, 2012), and land EM (e.g., Zhdanov et al., 2011c). As examples of our massively parallelized IE-based software, we present case studies for the inversion of (1) marine MT data from Gemini Prospect, Gulf of Mexico, and (2) AEM data from Ft. Yukon, Alaska, including the use of a moving sensitivity domain modified from Cox and Zhdanov (2007), and Cox et al. (2010).

**Gemini, marine MT**

Gemini Prospect is located about 200 km southeast of New Orleans in water about 1 km deep in the northern Gulf of Mexico. The salt body at Gemini Prospect has been determined by 3D seismic reflection survey, revealing a complex 3D salt structure at depths 1 to 5 km beneath the seafloor in 1 km deep water and has a high electrical resistivity compared with surrounding sediments (Key, 2003). In 1997, 1998, 2001, and 2003, MT data were collected at 42 sites in a two-dimensional (2D) grid over the Gemini salt body using broadband MT sensors developed by the Scripps Institution of Oceanography (Constable et al., 1998).

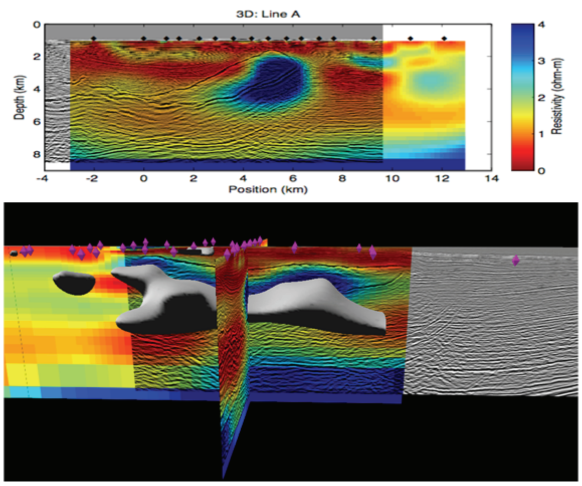


**Figure 1.** A vertical cross-section (top) and a 3D view (bottom) of the resistivity model overlapped with seismic sections.

We have inverted marine MT data (thirteen frequencies from 0.004005 to 1.0009 Hz) acquired over the Gemini Prospect, Gulf of Mexico. The 3D earth model spanned 16 km in the easting, 25 km in the northing, and 8 km with depth, and was discretized into cells of 125 m x 125 m dimension that were 50 m thick at the sea bottom and logarithmically increased with depth. In total, the model contained 1,638,400 cells.

The 3D resistivity model recovered from our inversion (Figure 1) resolves very clearly the shape and location of the salt-dome structure that was determined using 3D seismic prestack depth migration.

**Yukon, AEM**

Ft. Yukon is located at the confluence of the Yukon and Porcupine Rivers in the interior of Alaska. The area lies at the boundary of continuous and discontinuous permafrost. An 1800 line kilometre RESOLVE frequency domain survey was flown in the area to study the permafrost features in the area and create a groundwater model.

We have inverted RESOLVE (frequency-domain airborne system) acquired over the Ft. Yukon, Alaska. The RESOLVE data consisted of co-planar data acquired at 380 Hz, 1800 Hz, 8200 Hz, 40000 Hz, and 128000 Hz, and co-axial data acquired at 3300 Hz. The 3D earth model spanned 30 km in the inline direction, 10 km in the cross-line direction, and 140 m in depth. The cells were 15 m in the inline direction, 50 m in the cross-line direction, a varied from 1 m to 14 m in thickness. In total, the model contained 7.5 million active inversion cells.

The airborne data were gathered to study the creation and refreezing of taliks in interior Alaska. Areas of permafrost are shown as very resistive (dark blue), while unfrozen sands, silts, and clays are lower resistivity (reds and whites), in Figure 2. The town of Ft. Yukon was a no-fly zone, and is located at 580000mE and 7383000mN. There are many lakes in the area under which the soil is in various stages of freezing and thawing. The inversion results were used to model the thermodynamic evolution of these lakes and associated permafrost features.

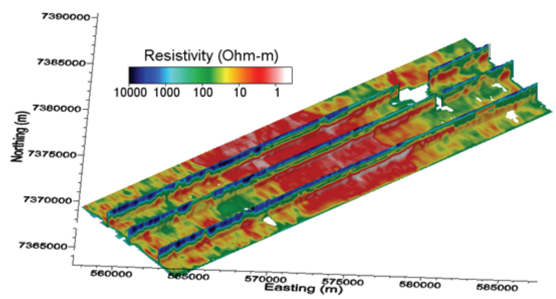


**Figure 2.** A prospective view of inverse 3D resistivity model.

## CONCLUSION

Over the last 40 years, the IE method has evolved from a purely academic technique into a practical method for mega-cell 3D modeling and inversion of land, borehole, marine, and airborne EM data. With advances in algorithms, software engineering, and computing resources, the IE method now has the same model complexity as any of the finite-difference or finite-volume methods, while providing efficient inversion algorithms. The advantage of the IE method is that it can be formulated to solve for the total field while using a distributed source term. This not only ensures an accurate solution for modeling, but provides a rapid and accurate means for computing sensitivities and/or adjoint operators required in 3D EM inversion. The IE method can also be used to incorporate the moving sensitivity domain, which provides the basis for extremely large scale airborne and marine EM data inversion.

## ACKNOWLEDGMENTS

The authors acknowledge TechnoImaging for support and permission to publish. Zhdanov and Čuma acknowledge support of the University of Utah's Consortium for Electromagnetic Modeling and Inversion (CEMI) and the Centre for High Performance Computing (CHPC). Scripps Institution of Oceanography and USGS are acknowledged for providing the marine and airborne EM data.

## REFERENCES

Avdeev, D. B., Kuvshinov, A. V., Pankratov, O. V., and Newman, G. A., 1997, High-performance three-dimensional electromagnetic modeling using modified Neumann Series: Wide-band numerical solution and examples, *J. Geomag. Geoelectr.*, **49**, 1519-1539.

Avdeev, D. B., Kushinov, A. V., Pankratov, O. V., and Newman, G. A., 2002, Three-dimensional induction logging problems, Part I: An integral equation solution and model comparisons, *Geophysics*, **67**, 413-426.

Constable, S. C., A. S. Orange, G. M. Hoversten, and H. F. Morrison, 1998, Marine magnetotellurics for petroleum exploration, part I: A sea-floor equipment system, *Geophysics*, **63**, 816-825.

Cox, L. H. and M. S. Zhdanov, 2007, Large-scale 3D inversion of HEM data using a moving footprint:, SEG 77th Annual Meeting, Expanded Abstracts, 467–470.

Cox, L. H., Wilson, G. A., and Zhdanov, M. S., 2010, 3D inversion of airborne electromagnetic data using a moving footprint, *Exploration Geophysics*, **41**, 250-259.

Dmitriev, V. I., and Nesmeyanova, N. I., 1992, Integral equation method in three-dimensional problems of low frequency electrodynamics (in Russian), Computat Math Model 3: 313.

Endo, M., Čuma, M., and Zhdanov, M. S., 2009, Multiple domain integral equation method for 3D electromagnetic modeling in complex geoelectrical structures, SEG 79th Annual Meeting, Expanded Abstracts, 679-683.

Hohmann, G. W., 1975, Three-dimensional induced polarization and electromagnetic modeling, *Geophysics*, **40**, 309-324.

Hursán, G., and Zhdanov, M. S., 2002, Contraction integral equation method in three-dimensional electromagnetic modeling, *Radio Science*, **37**, 1089-2002.

Key, K. W., 2003, Application of broadband marine magnetotelluric exploration to a 3-D salt structure and a fast spreading ridge, Ph. D. thesis, University of California, San Diego.

Raiche, A. P., 1974, An integral equation approach to three-dimensional modeling, *Geophys. J. R. Astr. Soc.*, **36**, 363-376.

Singer, B. S., and Fainberg, E. B., 1995, Generalization of the iterative dispersive method for modeling electromagnetic fields in nonuniform media with displacement currents, *J. App. Geophys.*, **34**, 41-46.

Wannamaker, P. E., 1991, Advances in three-dimensional magnetotelluric modeling using integral equations, *Geophysics*, **56**, 1716-1728.

Weidelt, P., 1975, Electromagnetic induction in three-dimensional structures, *J. Geophys.*, **41**, 85-109.

Xiong, Z., 1992, Electromagnetic modeling of 3-D structures by the method of system iteration using integral equations, *Geophysics*, **57**, 1556-1561.

Xiong, Z., and Tripp, A. C., 1995, A block iterative algorithm for 3-D electromagnetic modeling using integral equations with symmetrized substructures, *Geophysics*, **60**, 291-295.

Zhdanov, M. S., 2002, Geophysical inverse theory and regularization problems, Elsevier, Amsterdam.

Zhdanov, M. S., 2009, Geophysical electromagnetic theory and methods, Elsevier, Amsterdam.

Zhdanov, M. S., Lee, S. K., and Yoshioka, K., 2006, Integral equation method for 3D modeling of electromagnetic fields in complex structures with inhomogeneous background conductivity, *Geophysics*, **71**, G333-G345.

Zhdanov, M. S., Wan, L., Gribenko, A., Čuma, M., Key, K., and Constable, S., 2011a, Large-scale 3D inversion of marine magnetotelluric data: Case study from the Gemini prospect, Gulf of Mexico, *Geophysics*, **76**, F77-F87.

Zhdanov, M. S., Čuma, M., Wilson, G. A., Velikhov, E. P., Black, N., and Gribenko, A. 2011b, Iterative electromagnetic migration for 3D inversion of marine CSEM data, *Geophysical Prospecting*, **59**, 1101-1113.

Zhdanov, M. S., Smith, R. B., Gribenko, A., Čuma, M., and Green, M., 2011c, Three-dimensional inversion of large-scale EarthScope magnetotelluric data based on the integral equation method: Geoelectrical imaging of the Yellowstone conductive mantle plume, *Geophysical Research Letters*, **38**, L08307.

Zhdanov, M. S., Anderson, C., Endo, M., Cox, L. H., Čuma, M., Wilson, G. A., Black, N., and Gribenko, A., 2012, 3D inversion of towed streamer EM data: A model study of the Harding field with comparison to CSEM, *First Break*, **30**, 71-74.